Phospholamban Inhibits Ca-ATPase Conformational Changes Involving the E2 Intermediate†

Jason R. Waggoner,‡ Jamie Huffman,§ Jeffrey P. Froehlich,|| and James E. Mahaney*,⊥

Department of Pharmacology and Cell Biophysics, University of Cincinnati College of Medicine, Cincinnati, Ohio 45267, Department of Molecular Genetics and Biochemistry, University of Pittsburgh, Pittsburgh, Pennsylvania 15261, Department of Biochemistry and Molecular Biology, University of Maryland School of Medicine, Baltimore, Maryland 21201, and Virginia College of Osteopathic Medicine, 2265 Kraft Drive, Blacksburg, Virginia 24060

Received July 6, 2006; Revised Manuscript Received November 21, 2006

ABSTRACT: We have used steady-state fluorescence spectroscopy in combination with enzyme kinetic assays to test the hypothesis that phospholamban (PLB) stabilizes the Ca-ATPase in the E2 intermediate state. The cardiac muscle Ca-ATPase (SERCA2a) isoform was expressed either alone or coexpressed with PLB in High-Five insect cells and was isolated as insect cell microsomes. Fluorescence studies of the Ca-ATPase covalently labeled with the probe 5-(2-((iodoacetyl)amino)ethyl)aminonaphthalene-1-sulfonic acid showed that PLB decreased the amplitude of the Ca-ATPase E2 → E1 conformational transition by 45 ± 3% and shifted the [Ca^{2+}] dependence of the transition to higher Ca^{2+} levels (ΔK_{Ca} = 230 nM), similar to the effect of PLB on Ca-ATPase activity. Similarly, PLB decreased the amplitude of Ca-ATPase phosphorylation by inorganic phosphate (P_i) by 55 ± 2% and decreased slightly the affinity for P_i ($\Delta K_{0.5}$ = 70 μM). However, PLB did not affect the Ca^{2+}-dependent inhibition of Ca-ATPase phosphorylation by P_i. Finally, PLB decreased Ca-ATPase sensitivity to vanadate, increasing the IC_{50} value by 300 nM. The results suggest that PLB binding to Ca-ATPase stabilizes the enzyme in a conformation distinct from E2, decreasing the number of enzymes in the E2 state capable of undergoing ligand-dependent conformational changes involving the Ca-free E2 intermediate. The inability of conformation-specific ligands to fully convert this E2-like state into E1 or E2 implies that these states are not in a simple equilibrium relationship.

The sarcoplasmic reticulum (SR)[1] Ca-ATPase is a 110 kDa integral membrane protein that utilizes adenosine 5′-triphosphate (ATP) to drive the transport of Ca^{2+} ions into the SR to promote muscle relaxation (*1*, *2*). Phospholamban (PLB), a 52 amino acid phosphoprotein, is the principal regulator of the Ca-ATPase in cardiac SR (CSR) (*3*−*5*). Phosphorylation of PLB at Ser-16 or Thr-17 relieves Ca-ATPase inhibition, giving an increase in the rate of cardiac muscle relaxation as well as a positive inotropic effect (*6*−*8*). Abnormal Ca-ATPase regulation by PLB has been implicated as a causative factor for diastolic dysfunction, cardiac hypertrophy, and heart failure (*8*−*11*). Therefore, a key step in understanding important cardiac pathologies is elucidating the molecular details of the PLB−Ca-ATPase interaction (*7*, *11*).

PLB inhibits Ca-ATPase activity by decreasing the apparent Ca^{2+} affinity of the enzyme (*3*), but the physical basis of this effect is not fully understood. We have reported (*12*) that PLB prevents intermolecular coupling of Ca-ATPase units within an oligomeric complex, which is essential for the activated Ca^{2+} transport activity observed when PLB inhibition is relieved. While inhibitory PLB binding to the enzyme may physically block one (or more) oligomer contact site(s) on the enzyme, preventing Ca-ATPase oligomerization, it is also possible that PLB binding to one (or both) subunit(s) may induce an enzyme conformational state that does not readily form conformationally and chemically coupled oligomers (*13*, *14*). Under physiological conditions, PLB remains associated with Ca-ATPase at all times, even in the presence of saturating Ca^{2+} (*15*, *16*), where PLB inhibition of Ca-ATPase activity is less pronounced (*12*), and following PLB phosphorylation (*16*), which relieves PLB inhibition of Ca-ATPase. Nevertheless, PLB inhibition of Ca-ATPase is particularly potent when [Ca^{2+}] is low (*3*), suggesting that the key inhibitory interaction between PLB and Ca-ATPase occurs preferentially for the E2 (Ca^{2+}-free) rather than the E1 (Ca-bound) conformation of the enzyme (*18*−*20*). Indeed, initial modeling studies (*21*, *22*) proposed

† This work was supported by grants from the American Heart Association to J.R.W. (AHA 0215055B), J.P.F. (AHA 0555534U), and J.E.M. (AHA 0040094N).

* To whom correspondence should be addressed: Virginia College of Osteopathic Medicine, 2265 Kraft Drive, Blacksburg, VA 24060. Telephone: (540) 231-1948. Fax: (540) 231-8846. E-mail: jmahaney@vcom.vt.edu.

‡ University of Cincinnati College of Medicine.

§ University of Pittsburgh.

|| University of Maryland School of Medicine.

⊥ Virginia College of Osteopathic Medicine.

[1] Abbreviations: SR, sarcoplasmic reticulum; SERCA, sarco(endo)-plasmic reticulum Ca-transporting adenosine triphosphosphatase; PLB, phospholamban; CSR, cardiac sarcoplasmic reticulum; HF, High-Five; 2D12, anti-PLB monoclonal antibody; ATP, adenosine 5′-triphosphate; IAEDANS, 5-(2-((iodoacetyl)amino)ethyl)aminonaphthalene-1-sulfonic acid; EGTA, ethylenebis(oxyethylenenitrilo)tetraacetic acid; MOPS, 3-(*N*-morpholino)propanesulfonic acid; EP, phosphoenzyme; P_i, inorganic phosphate.

10.1021/bi061365k CCC: $37.00
Published on Web 01/30/2007

putative inhibitory binding sites for PLB on the E2 form of the Ca-ATPase that are not present on the E1 form of the enzyme. These early models were updated recently by Zamoon et al. (*23*), who used magnetic resonance techniques to determine the orientation of PLB bound to its inhibitory site on the Ca-ATPase E2 form, which they confirmed fit better on the E2 structure than the E1·Ca_2 structure. Finally, Li et al. (*24*−*26*) used fluorescence techniques to determine the time-averaged structural orientations of the Ca-ATPase and PLB when bound as an inhibitory complex and when separated. The authors proposed that inhibitory PLB binding to the Ca-ATPase induces a 10° reorientation of the N domain (*27*, *28*) toward the bilayer to bring known interaction sites between PLB and Ca-ATPase into proximity (cf. Figure 8 of ref *26*). This suggests the PLB-inhibited Ca-ATPase is in an intermediate conformation between the more compact E2 and open E1·Ca_2 structures (*28*). The Ca-ATPase inhibition studies of Mahaney et al. (*29*) support this model, by showing that PLB decreases Ca-ATPase sensitivity to thapsigargin (TG), which binds specifically to the Ca-ATPase E2 conformation to form the E2·TG structure (*28*). Additional studies are needed to characterize the unique physical and kinetic properties of the PLB-inhibited Ca-ATPase conformation to determine the relationship of the PLB-inhibited Ca-ATPase conformation to the Ca^{2+}-free E2 and calcium-bound E1 forms of the enzyme.

Therefore, in the present study, we investigated the effects of PLB on the Ca-ATPase E2 conformational state by measuring the enzyme transitions involving the E2 state. We used steady-state fluorescence spectroscopy to measure the [Ca^{2+}]-dependent Ca-ATPase E2 → E1 transition and ^{32}P-inorganic phosphate to measure the Ca-ATPase E2 → E2P transition. Additional measurements were made using the inhibitor vanadate, to test Ca-ATPase sensitivity to an inhibitory agent that binds specifically to the E2 state. For this work, we used the baculovirus High-Five (HF) insect cell expression system to produce cellular microsomes containing the Ca-ATPase [the sarco(endo)plasmic reticulum Ca-transporting adenosine triphosphotase (SERCA2a) isoform] expressed alone or coexpressed with PLB (*30*). The functional (*30*), physical (*31*), and kinetic (*12*) properties of the coexpressed Ca-ATPase and PLB in the insect cell microsomal environment are nearly identical to those of Ca-ATPase and PLB in native CSR vesicles. Use of this expression system facilitated the direct comparison of the Ca-ATPase in the absence or presence of PLB while alleviating the need to physically uncouple PLB from the Ca-ATPase (i.e., PLB phosphorylation or treatment of the sample with an anti-PLB monoclonal antibody). The results of our study show that PLB decreased the amplitude of conformational transitions involving the E2 state and decreased the apparent enzyme affinity for Ca^{2+}, inorganic phosphate (P_i), and vanadate. The results are discussed in terms of the model of Li et al. (*26*), in which PLB stabilizes the Ca-ATPase in an E2-like state, "E", intermediate between E2 and E1·Ca_2, resulting in a decrease in the apparent affinity of the enzyme for Ca^{2+}, P_i, and inhibitors that bind specifically to the E2 conformation.

EXPERIMENTAL PROCEDURES

Materials. 5-(2-((Iodoacetyl)amino)ethyl)aminonaphthalene-1-sulfonic acid (IAEDANS) was purchased from Molecular Probes. [^{32}P]H_3PO_4 was purchased from MP Biomedicals, and ^{125}I-labeled protein A was purchased from Perkin-Elmer Life Sciences. Sodium vanadate was purchased from Sigma. Prestained molecular-weight standards and polyvinylidene difluoride (PVDF) membranes were purchased from Bio-Rad. The Bac-to-Bac baculovirus expression system and HF insect cells were purchased from Invitrogen. All other reagents were of the highest purity available.

Protein Expression, Isolation, and Characterization. Canine cardiac Ca-ATPase (the SERCA2a iosform) and canine PLB were coexpressed in HF cells as reported elsewhere (*30*). Microsomes were harvested 48 h after baculovirus infections and stored in small aliquots at −50 °C. Protein concentrations were determined by the method of Lowry et al. (*32*), using bovine serum albumin (Sigma) as a standard. The amount of SERCA2a and PLB in the microsomes was quantified by gel electrophoresis and immunoblotting, using methods described previously (*30*). Several different preparations of expressed SERCA2a without or with coexpressed PLB were used in these studies. The Ca-ATPase content of the microsomes was very carefully matched at 16% of the total protein by weight, and the relative proportion of Ca-ATPase to PLB coexpressed in the microsomes was between 1 and 2 mol of PLB/mol of Ca-ATPase (*30*). For all preparations, the Ca-ATPase was under full regulatory control by PLB when the two proteins were coexpressed, determined by assays of [Ca^{2+}]-dependent ATPase and Ca-uptake activity conducted in the presence and absence of anti-PLB antibody, as reported previously for these samples (*30*).

SERCA2a ATPase Assay and Inhibition Studies. [Ca^{2+}]-Dependent ATPase activity of SERCA2a in the HF insect cell microsomes was measured colorimetrically using a malachite green-ammonium molybdate assay as previously described (*33*). SERCA2a incubation tubes contained 0.05 mg/mL protein in 50 mM 3-(*N*-morpholino)propanesulfonic acid (MOPS) (pH 7.0), 3 mM $MgCl_2$, 100 mM KCl, 1 mM ethylenebis(oxyethylenenitrilo)tetraacetic acid (EGTA), and 0−1.0 mM $CaCl_2$ to give the desired ionized [Ca^{2+}], as previously determined (*34*). To initiate the ATPase reaction, 5 mM MgATP was added to the incubation tube at 37 °C. SERCA2a samples were pretreated with 20 μg of the Ca^{2+} ionophore A23187/mg of total protein to prevent Ca^{2+} build-up within the microsome during the assay. The [vanadate] dependence of SERCA2a inhibition was measured at 37 °C using the malachite green-ammonium molybdate assay essentially as described above. SERCA2a incubation tubes contained 0.05 mg/mL protein in 50 mM MOPS (pH 7.0), 3 mM $MgCl_2$, 100 mM KCl, 1 mM EGTA, and 0.7 mM $CaCl_2$ (final ionized [Ca^{2+}] = 625 nM), and [vanadate] as indicated. A 10 mM stock solution of vanadate in water was prepared according to Goodno (*35*) and stored at 4 °C until use. Serial dilutions were made to provide the desired level of vanadate for each experiment.

Labeling of Ca-ATPase with IAEDANS. SERCA2a expressed in insect cell microsomes was labeled by IAEDANS according to Obara et al. (*36*) with substantial modifications. Prior to each labeling procedure, a fresh stock of IAEDANS was prepared from powder, using *N*,*N*-dimethylformamide (DMF) as the solvent. The microsomes (5 mg/mL) were labeled with 85 μM IAEDANS in the presence of labeling buffer (20 mM MOPS, 80 mM KCl, 1 mM $CaCl_2$, and 5

mM $MgCl_2$) and 5 mM ATP at pH 6.88 for 30 min at room temperature. Excess reagent was removed by centrifugation for 30 min at 30 000 rpm (70000*g*), 4 °C, in a Beckman Ti45 rotor. The pellet, containing the AEDANS-labeled SERCA2a (henceforth denoted AEDANS-SERCA2a), was resuspended in 0.3 M sucrose, 20 mM MOPS, and 0.1 mM $CaCl_2$ (pH 7.0). The stoichiometry of AEDANS bound per SERCA2a was determined in a solution of 1% sodium dodecyl sulfate (SDS) in 0.1 M NaOH, using an extinction coefficient of 6.1×10^3 M^{-1} cm^{-1} at 340 nm (*36*). The amount of SERCA2a in the sample was quantified separately by a protein assay and quantitative immunoblot, as described above. The labeling protocol used was developed by constructing labeling curves (data not shown) to determine the relationship between the concentration of IAEDANS added to the microsome incubation mixture, the resultant ratio of bound AEDANS to enzyme, and ATPase activity at each labeling level (cf. Figure 1 in ref *13*).

Fluorescence Measurements. Measurements of the fluorescence intensity were performed at 25 °C using a Photon Technology International QM-2000-4 spectrofluorimeter equipped with a cuvette stirrer. Excitation and emission spectra of the AEDANS−Ca-ATPase showed optimal excitation and emission wavelengths of 352 and 475 nm, respectively (data not shown).

To measure fluorescence intensity changes following a $[Ca^{2+}]$ jump, insect cell microsomes containing AEDANS-SERCA2a (0.35 mg/mL) were suspended in a standard buffer (50 mM MOPS at pH 7.0, 100 mM KCl, and 3 mM $MgCl_2$) and either 1 mM EGTA and no added $CaCl_2$ ($[Ca^{2+}]_{free} \sim 0$), designed to favor the formation of the Ca-free E2 state initially, or ~15 μM Ca^{2+}, designed to favor the formation of the calcium-bound E1·Ca_2 state initially. The addition of 1.25 mM Ca^{2+} to the standard buffer containing 1 mM EGTA with no added $CaCl_2$ (final $[Ca^{2+}]_{free} \sim 250$ μM) promoted the formation of the E1·Ca_2 conformation, whereas the addition of 1.25 mM EGTA to the standard buffer with ~15 μM Ca^{2+} (final $[Ca^{2+}]_{free} \sim 0$ μM) promoted the formation of the E2 conformation. The fluorescence intensity was measured by summing the total fluorescence emission over 20 s before (initial fluorescence intensity, F_o) and after (final fluorescence intensity, F) the respective additions. Fluorescence intensity changes were quantified as percent changes, according to the formula $100 \times (F - F_o)/F_o$.

To measure incremental $[Ca^{2+}]$-dependent fluorescence changes, microsomal AEDANS−Ca-ATPase (0.35 mg/mL) was suspended in the standard buffer containing 1 mM EGTA and no added $CaCl_2$ ($[Ca^{2+}]_{free} \sim 0$ μM), which favored the formation of the E2 state. The initial fluorescence intensity (F_o) of the sample was measured, and then $CaCl_2$ was added in 0.1 mM increments up to 1 mM final Ca^{2+}, which provided $[Ca^{2+}]_{free}$ between 30 nM and 15 μM. The total volume of $CaCl_2$ added was 20 μL, which had a negligible effect on the total sample volume (2 mL total). After each Ca^{2+} addition, the fluorescence emission was averaged over a 20 s period and expressed as the percent change from the initial fluorescence level (F_o) as described above.

The effect of the nonhydrolyzable ATP analogue AMPPNP on AEDANS-SERCA2a fluorescence intensity was measured using microsomes containing AEDANS-SERCA2a (0.35 mg/mL) suspended in standard buffer containing 1.25 mM $CaCl_2$ ($[Ca^{2+}]_{free} \sim 15$ μM), which favored the formation of the Ca-bound E1·Ca_2 state. The initial fluorescence intensity (F_o) of the sample was measured, and AMPPNP was added to a final concentration of either 50 μM, 0.5 mM, or 5 mM to promote the formation of the E1·Ca_2·AMPPNP intermediate state. The fluorescence emission was averaged over 20 s after the AMPPNP addition and expressed as the percent change from the initial fluorescence level (F_o) as described above.

Phosphoenzyme (EP) Formation from P_i. $[P_i]$-Dependent SERCA2a EP formation was carried out at 25 °C using insect cell microsomes (1.0 mg/mL) suspended in a solution containing 10 mM $MgCl_2$, 1 mM EGTA and no added $CaCl_2$ ($[Ca^{2+}]_{free} \sim 0$), and 50 mM 2-(*N*-morpholino)ethanesulfonic acid (MES) at pH 6.0. To initiate phosphorylation, an equal volume of the same buffer containing variable amounts of $[^{32}P]Na_2HPO_4$ (0−8 mM final concentration) was added to the microsomes and vortexed. After 15 min of incubation, the reaction was quenched by the addition of 3% perchloric acid plus 2 mM H_3PO_4 (final concentrations). Bovine serum albumin (0.25 mg) was added to each sample as a carrier protein. The quenched vesicles were pelleted in a tabletop centrifuge and then washed 3 times with a solution of 5% trichloroacetic acid, 4 mM H_3PO_4 (nonradio-labeled), and 6% polyphosphoric acid. The final pellets were dissolved in 5 mL of 1 N NaOH, and the $[^{32}P]$ EP was assayed by scintillation counting. To measure $[Ca^{2+}]$-dependent inhibition of SERCA2a EP formation by P_i, microsomes (1.0 mg/mL) were suspended in a solution containing 10 mM $MgCl_2$, 1 mM EGTA and no added $CaCl_2$ ($[Ca^{2+}]_{free} \sim 0$), and 50 mM MES at pH 6.0. To initiate phosphorylation, an equal volume of the same buffer containing 4 mM $[^{32}P]Na_2HPO_4$ and variable $[CaCl_2]$ from 0 to 1.2 mM (final concentrations) were added to the microsomes, providing ionized $[Ca^{2+}]$ levels of 0−200 μM in the reaction mixture. After a 15 min incubation period at 25 °C, the reaction was quenched and the microsomes were washed and processed as described above.

Curve Fitting and Error Analysis. Experimental data were fitted using KFIT written by N. C. Millar, which was obtained from Dr. Carl Frieden via his website: www.wuarchive.wustl.edu/packages/kinsim/uploads. The best fits of the data were chosen on the basis of the minimization of the sum-of-squares error, χ^2. Results are expressed as mean ± standard errors. Statistical analysis was performed with the use of the two population Student's *t* test. Values of $p < 0.05$ are considered to be significantly different.

RESULTS

Protein Expression and Characterization. HF insect cell microsomes containing expressed SERCA2a minus PLB and SERCA2a plus PLB used for this study were produced and characterized previously (*30*). The SERCA2a coexpressed with PLB was under the full regulatory control of PLB, which increased the $K_{0.5}$ for the high-affinity Ca^{2+} transport sites relative to SERCA2a without PLB and for PLB uncoupled from SERCA2a following treatment of the SERCA2a plus PLB samples with the anti-PLB monoclonal antibody 2D12 (*30*, *37*). Further information regarding the physical and kinetic characteristics of the expressed samples, including the expression−activity properties, has been published previously (*12*, *30*).

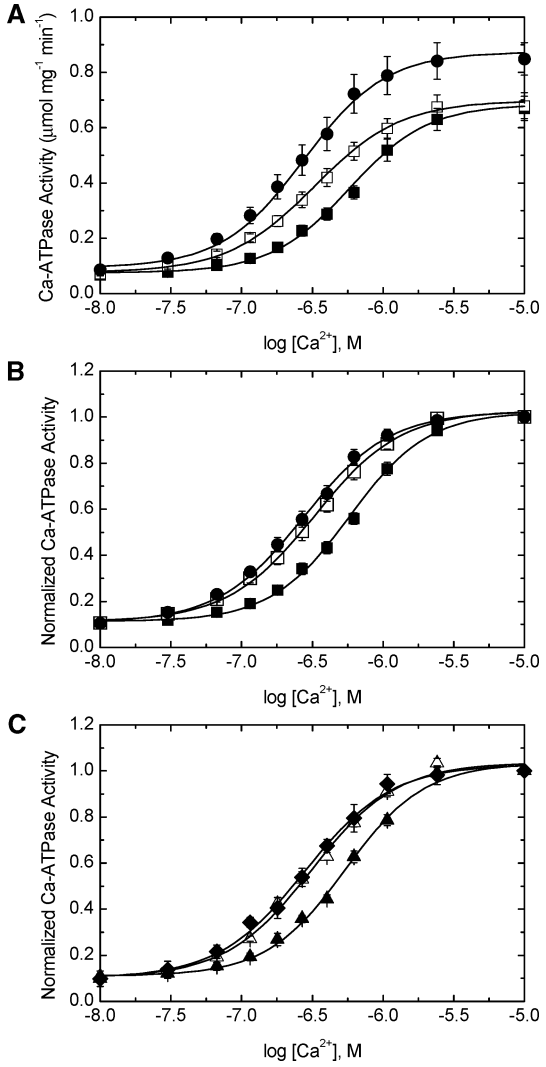

FIGURE 1: Effect of PLB on the $[Ca^{2+}]$-dependent Ca-ATPase activity of expressed SERCA2a in HF insect cell microsomes at 37 °C. (A) Control, unlabeled microsomes (0.05 mg of total protein/mL) containing SERCA2a alone (●) or SERCA2a plus PLB (■) were assayed in a medium (henceforth designated "standard buffer") containing 50 mM MOPS at pH 7.0, 3 mM Mg_2Cl, 100 mM KCl, 1 mM EGTA, and 0−1.0 mM $CaCl_2$ to give the desired ionized $[Ca^{2+}]$, as previously determined (*30*). Each assay was initiated by the addition of 5 mM MgATP to the incubation tube. The microsomes were pretreated with 20 μg of A23187/mg of protein in the incubation medium to prevent Ca^{2+} accumulation in the microsomes. The SERCA2a content of each sample was matched at 16% (Table 1), which facilitated a direct comparison of the activity data. To assess the inhibitory effect of PLB on Ca-ATPase activity, a SERCA2a plus PLB sample was incubated for 20 min on ice with anti-PLB monoclonal antibody 2D12 at an antibody/protein weight ratio of 1:1 (*30*) prior to the assay (□). Calcium-dependent SERCA2a ATPase and Ca^{2+} uptake activity data were fit to the Hill equation using KFIT (*30*) to generate values for K_{Ca} and V_{max} (Table 1). (B) Each curve in A was normalized to its maximum value, to more clearly demonstrate the effects of treating the SERCA2a plus PLB sample (■) with an anti-PLB monoclonal antibody (□) to uncouple PLB from SERCA2a. (C) Ca-ATPase activity data from IAEDANS-labeled SERCA2a in the absence (◆) and presence (▲) of PLB and in the presence of PLB following treatment with anti-PLB monoclonal antibody (△), each normalized to their respective maximum value. Symbols represent the average of five repetitions, and error bars correspond to the standard error of the mean for each point.

Figure 1A shows the $[Ca^{2+}]$-dependent ATPase activity for the expressed samples at 37 °C. In the absence of PLB,

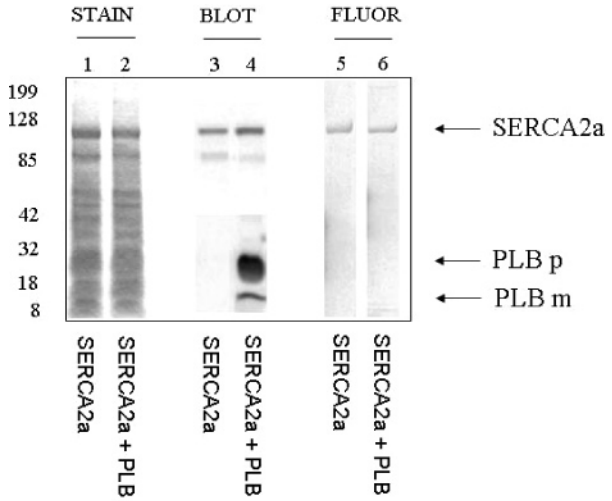

FIGURE 2: Analysis of AEDANS-SERCA2a in HF insect cell microsomes. Insect cell microsomes containing SERCA2a alone (lanes 1, 3, and 5) or SERCA2a plus PLB (lanes 2, 4, and 6) were labeled with IAEDANS and analyzed by SDS−PAGE and immunoblotting as described in the Experimental Procedures. Lanes 1 and 2, GelCode Blue-stained gel; lanes 3 and 4, corresponding immunoblot of the samples; and lanes 5 and 6, negative image photograph of the SERCA2a samples illuminated by a UV light source.

the SERCA2a activity curve (● in Figure 1) was shifted to the left (ΔK_{Ca} = 300 nM) relative to SERCA2a plus PLB (■ in Figure 1) and had a 27% larger V_{max} compared to the SERCA2a plus PLB sample. Pretreatment of the SERCA2a plus PLB sample with anti-PLB antibody (□ in Figure 1) increased the apparent Ca^{2+} affinity of the enzyme compared to that of SERCA2a in the absence of PLB but did not increase V_{max} compared to the untreated SERCA2a plus PLB sample (■ in Figure 1). The samples used in this experiment were carefully matched for SERCA2a content (∼16% by weight total protein, see the Experimental Procedures), indicating that the differences in V_{max} for the SERCA2a minus PLB sample versus the SERCA2a plus PLB sample were not due to different Ca-ATPase levels in the two samples. Likewise, our previous kinetics studies showed that these differences do not arise from differences in the amount of active expressed SERCA2a in the two sample types (*12*, *30*). Figure 1B shows each curve normalized to its maximum value to more clearly demonstrate that uncoupling PLB from SERCA2a with an anti-PLB monoclonal antibody (□ in Figure 1B) produces a $[Ca^{2+}]$ dependence similar to that observed for SERCA2a in the absence of PLB (● in Figure 1B).

Fluorescence Studies of IAEDANS-Labeled SERCA2a. Insect cell microsomes containing expressed SERCA2a alone or SERCA2a coexpressed with PLB were labeled with the fluorescent probe IAEDANS (henceforth denoted AEDANS-SERCA2a) and analyzed by SDS−polyacrylamide gel electrophoresis (PAGE) (Figure 2). The gels indicate a single major band containing the bound fluorescence probe, which corresponds to the SERCA2a protein band. The fluorescence images (lanes 5 and 6) show a diffuse fluorescence in the lower left region of the lanes. This was due to sample bleed-through from the adjacent left-hand lanes on the original gel (not shown in the figure), which contained comparative microsomal samples that were incubated with IAEDANS but not yet washed to remove the unbound label. The stoichi-

Table 1: Characterization of SERCA2a and PLB Coexpressed in HF Insect Cells[a]

	expression		SERCA2a ATPase activity, at 37 °C			
sample type	SERCA2a (wt % total protein)	PLB (wt % total protein)	V_{max} −Ab [μmol (mg of protein)$^{-1}$ min^{-1}]	V_{max} +Ab [μmol (mg of protein)$^{-1}$ min^{-1}]	K_{Ca} −Ab (μM)	K_{Ca} +Ab (μM)
SERCA2a alone	15.7 ± 0.6	0.00	0.88 ± 0.06	0.91 ± 0.07	0.29 ± 0.07	0.28 ± 0.08
AEDANS-SERCA2a alone			0.84 ± 0.05	nd	0.29 ± 0.09	nd
SERCA2a plus PLB	15.8 ± 0.7	1.42 ± 0.1	0.71 ± 0.03	0.73 ± 0.04	0.60 ± 0.08	0.35 ± 0.05
AEDANS-SERCA plus PLB			0.65 ± 0.03	0.66 ± 0.04	0.60 ± 0.07	0.34 ± 0.06

[a] SERCA2a and PLB were coexpressed using the baculovirus HF insect cell expression system and isolated as insect cell microsomes, as previously reported (*30*). Three separate preparations each of SERCA2a alone and SERCA2a plus PLB from Waggoner et al. (*30*) were used for this study. Protein expression was determined by quantitative immunoblotting, using purified SERCA2a and purified PLB as standards. Using the molecular weight of 110 000 g/mol for Ca-ATPase and 6080 g/mol for PLB, the PLB/SERCA2a molar stoichiometry was determined to be 1.3 ± 0.1:1. [Ca^{2+}]-Dependent ATPase activity was assayed by inorganic phosphate liberation at 37 °C. For comparison, similar activity assays were conducted for expressed SERCA2a labeled with the fluorescent probe IAEDANS (AEDANS-SERCA2a). The functional effects of PLB on SERCA2a activity were determined by preincubating the samples in the absence (−Ab) or presence (+Ab) of the anti-PLB monoclonal antibody 2D12 prior to the activity assay. The maximum activity (V_{max}) and [Ca^{2+}] required for half-maximal activity (K_{Ca}) were determined from Hill fits of the [Ca^{2+}]-dependent ATPase activity for each sample. Additional characterization of the unlabeled samples is presented in refs *12* and *30*. Values represent the mean of three separate preparations each of SERCA2a alone and SERCA2a plus PLB, and the errors represent the standard error of the mean. nd = not determined.

ometry of SERCA2a labeling by IAEDANS was approximately 1 mol of the probe/1 mol of SERCA2a, determined by ultraviolet (UV) spectroscopic analysis of the bound probe and protein concentration corrected for the content of SERCA by weight determined by immunoblotting (see the Experimental Procedures). Using this analysis, we found no difference in IAEDANS labeling stoichiometry for SERCA2a in the absence or presence of PLB. The results indicated that the expressed SERCA2a was the only protein in the insect cell microsome that was significantly labeled by IAEDANS. Obara et al. (*36*) reported that IAEDANS binds the skeletal muscle Ca-ATPase (SERCA1) predominantly at Cys-674, a site that is conserved in SERCA2a, which shares 84% sequence identity and greater than 90% sequence homology with SERCA1 (*2*). However, a detailed sequence analysis to determine the site(s) of IAEDANS labeling on the expressed SERCA2a was not carried out. Because of this, our interpretation of fluorescence changes was limited to large scale conformational changes rather than sequence- of domain-specific motions.

The [Ca^{2+}]-dependent Ca-ATPase activity profiles of the microsomal AEDANS-SERCA2a samples were measured at 37 °C to facilitate a direct comparison with the unlabeled microsomes. The activity curves were nearly identical to that of the unlabeled samples, except that the labeled samples had approximately 5−10% lower V_{max} values relative to their unlabeled counterparts (Table 1). The data are shown normalized in Figure 1C to allow for a direct comparison of the individual samples. Control experiments in our laboratory (not shown) indicated that the loss of enzyme activity following IAEDANS labeling arose primarily from the physical handling of the sample during the centrifugation and resuspension steps needed to remove the unbound label, rather than from the labeling reaction itself. Thus, labeling SERCA2a with IAEDANS did not significantly affect the enzyme or the functional effects of PLB on the enzyme.

The fluorescence emission intensity of IAEDANS bound to SERCA2a is sensitive to the Ca-ATPase E2 → E1·Ca_2 conformational transition (*36*, *38*, *39*). To test the effect of PLB on the E2 → E1·Ca_2 equilibrium distribution, we measured [Ca^{2+}]-dependent fluorescence changes in AEDANS-

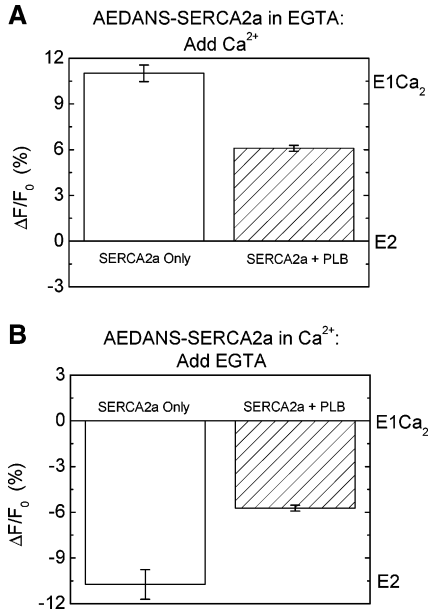

FIGURE 3: Effect of PLB on [Ca^{2+}]-jump-dependent fluorescence intensity changes of AEDANS-SERCA2a at 25 °C. (A) Insect cell microsomes (0.35 mg of total protein/mL) containing either AEDANS-SERCA2a expressed alone (open bars) or with PLB (hatched bars) were suspended in standard buffer containing 1 mM EGTA without added Ca^{2+} ([Ca^{2+}]$_{free}$ ∼ 0) to stabilize SERCA2a in the Ca^{2+}-free state. The steady-state fluorescence intensity was recorded prior to and following the addition of 1.25 mM $CaCl_2$ (final [Ca^{2+}]$_{free}$ ∼ 250 μM), and the [Ca^{2+}]-dependent change in fluorescence (ΔF) was divided by the initial fluorescence reading (F_o) and expressed as a percentage. (B) Experiment in A was repeated, except that the AEDANS-SERCA2a samples were first suspended in standard buffer containing [Ca^{2+}]$_{free}$ ∼ 15 μM to promote the formation of the E1·Ca_2 state and the steady-state fluorescence was measured before and after the addition of 1.25 mM EGTA (final [Ca^{2+}]$_{free}$ ∼ 0). Values represent the average of six independent experiments, and error bars represent the standard error of the mean.

SERCA2a alone or coexpressed with PLB in insect cell microsomes. These experiments were carried out at 25 °C to increase the resolution of the fluorescence signals. In the first experiment (Figure 3A), samples were preincubated in 1 mM EGTA with no added Ca^{2+} ([Ca^{2+}]$_{free}$ ∼ 0) to promote the formation of the Ca^{2+}-free E2 state initially. After a

$[Ca^{2+}]$ jump of 1.25 mM ($[Ca^{2+}]_{free} \sim 250$ μM), the fluorescence intensity of AEDANS-SERCA2a increased by $11 \pm 0.5\%$ ($n = 6$), whereas the fluorescence intensity of the AEDANS-SERCA2a plus PLB sample increased by only $6.1 \pm 0.2\%$ ($n = 6$). Thus, the presence of PLB decreased the amplitude of the E2 → E1·Ca_2 conformational transition by 45% ($p < 0.05$). In a parallel experiment (Figure 3B), samples were preincubated at $[Ca^{2+}]_{free} \sim 15$ μM to promote the formation of the Ca^{2+}-saturated E1·Ca_2 state initially. After the addition of 1.25 mM EGTA ($[Ca^{2+}]_{free} \sim 0$), the fluorescence intensity of AEDANS-SERCA2a alone decreased by $10.7 \pm 1.0\%$ ($n = 6$), whereas the fluorescence intensity of the AEDANS-SERCA2a plus PLB sample decreased by only $5.7 \pm 0.2\%$ ($n = 6$). The fluorescence intensity changes measured for the IAEDANS-labeled expressed SERCA2a in the absence of PLB are quantitatively similar to previous papers for AEDANS-SERCA1 in native skeletal SR vesicles (*36*, *38*), confirming that AEDANS-SERCA2a is the source of the $[Ca^{2+}]$-dependent changes that we measured. Therefore, the presence of PLB decreased the E1·Ca_2 → E2 conformational shift by 46% ($p < 0.05$), similar to the result of the first experiment (Figure 3A). The results indicate that the presence of PLB shifts the equilibrium distribution of AEDANS−Ca-ATPase in the direction of E2, thereby reducing the number of enzyme units undergoing the E2 → E1·Ca_2 transition (Figure 3A) and the E1·Ca_2 → E2 transition (Figure 3B). This result is similar to the activity data in Figure 1A, which also showed a PLB-dependent effect on SERCA2a V_{max} activity at saturating $[Ca^{2+}]$.

After we found an effect of PLB on the *amplitude* of the SERCA2a E2 → E1·Ca_2 transition, our second fluorescence experiment tested the effect of PLB on the *$[Ca^{2+}]$ dependence* of the E2 → E1·Ca_2 conformational transition. AEDANS-SERCA2a samples were preincubated in experimental buffer containing 1 mM EGTA and no added $CaCl_2$ ($[Ca^{2+}]_{free} \sim 0$) to promote the formation of the E2 state, and changes in the fluorescence intensity of AEDANS-SERCA2a were measured during the stepwise addition of calcium to the samples. The $[Ca^{2+}]$-dependent fluorescence changes of each sample type displayed a sigmoidal increase with increasing $[Ca^{2+}]$ (Figure 4A). As observed in the $[Ca^{2+}]$-jump experiment (Figure 3), there was a significant 38% ($p < 0.05$) difference between the maximum levels of fluorescence intensity change between AEDANS-SERCA2a only [$9.1 \pm 0.1\%$ ($n = 4$)] and AEDANS-SERCA2a plus PLB [$5.7 \pm 0.4\%$ ($n = 4$)] samples. As shown in the plot of the normalized data (Figure 4B), PLB also shifted the $[Ca^{2+}]$-dependent fluorescence intensity of AEDANS-SERCA2a to the right ($\Delta K_{Ca} = 210$ nM) relative to AEDANS-SERCA2a in the absence of PLB, similar to the PLB-dependent shift in AEDANS-SERCA2a Ca-ATPase activity, suggesting a direct correlation between the effect of PLB on the SERCA2a E2 → E1·Ca_2 conformational transition and SERCA2a activity. Thus, PLB decreases Ca-ATPase apparent Ca^{2+} affinity, at least in part, by reducing the number of enzyme units that can form the E1·Ca_2 intermediate state.

Finally, we tested the effect of PLB on the SERCA2a conformational change that accompanies ATP binding to E1·Ca_2 to form E1·Ca_2·ATP (*34*) and activates the enzyme for ATP-dependent EP formation (*40*). For these experiments, AEDANS-SERCA2a was preincubated with Ca^{2+} ($[Ca^{2+}]_{free}$

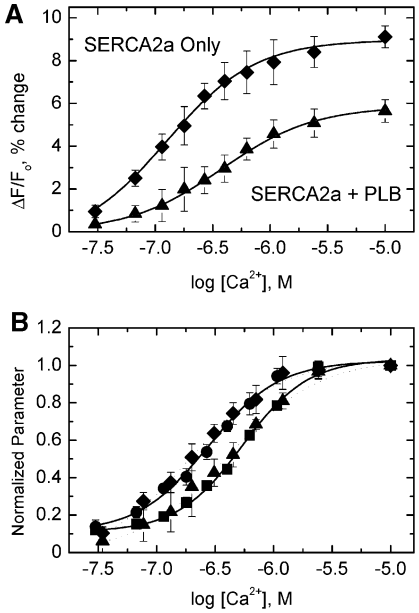

FIGURE 4: Effect of PLB on the $[Ca^{2+}]$ dependence of AEDANS-SERCA2a fluorescence intensity at 25 °C. (A) Insect cell microsomes containing either AEDANS-SERCA2a alone (◆) or AEDANS-SERCA2a plus PLB (▲) were incubated in standard buffer containing 1 mM EGTA and 0 added $CaCl_2$ ($[Ca^{2+}]_{free} \sim 0$), and $CaCl_2$ was added in 0.1 mM increments up to 1 mM final Ca^{2+} (~15 μM ionized Ca^{2+}). After each addition of calcium, the resulting increase in IAEDANS fluorescence intensity (F_i) was recorded and plotted as a percent change relative to the initial fluorescence in the absence of Ca^{2+} (F_o). The data were fit by the Hill equation using KFIT (*30*) to generate values for K_{Ca} and the maximum fluorescence change. (B) Fluorescence intensity data from A was normalized to each respective maximum value to provide a clearer comparison of the PLB-dependent shift and overlaid with the PLB-dependent changes in the $[Ca^{2+}]$ dependence of AEDANS-SERCA2a activity (SERCA2a alone, ●; SERCA2a plus PLB, ■) from Figure 1C. Symbols represent the average of four separate experiments, and error bars represent the standard error of the mean.

~ 15 μM) to promote the E1·Ca_2 state and fluorescence intensity changes following the addition of the nonhydrolyzable ATP analogue AMPPNP were recorded. The addition of AMPPNP to the AEDANS-SERCA2a samples resulted in a [AMPPNP]-dependent increase in fluorescence intensity, similar to that reported by Obara et al. (*36*). Three concentrations of AMPPNP were utilized (Figure 5): 50 μM to study high-affinity nucleotide-binding effects, an intermediate level of 0.5 mM, and a saturating level of 5 mM. The addition of 50 μM AMPPNP to microsomes containing AEDANS−Ca-ATPase only (open bars in Figure 5) increased the fluorescence intensity by $0.35 \pm 0.09\%$ ($n = 6$), whereas the increase in the AEDANS-SERCA2a plus PLB sample (hatched bars in Figure 5) was $1.2 \pm 0.3\%$ ($n = 6$). The addition of 0.50 mM AMPPNP to the AEDANS-SERCA2a only sample enhanced the fluorescence intensity by $1.0 \pm 0.06\%$ ($n = 6$) compared to a change of $3.1 \pm 0.3\%$ ($n = 6$) for the AEDANS-SERCA2a plus PLB sample. Finally, the addition of 5 mM AMPPNP to the AEDANS-SERCA2a sample resulted in a $6.7 \pm 0.2\%$ ($n = 6$) change in fluorescence, compared to the AEDANS-SERCA2a plus PLB sample, which changed by $8.3 \pm 0.2\%$ ($n = 6$). The fluorescence intensity changes at each AMPPNP level were significantly different ($p < 0.05$) between the AEDANS-SERCA2a only and the AEDANS-SERCA2a plus PLB

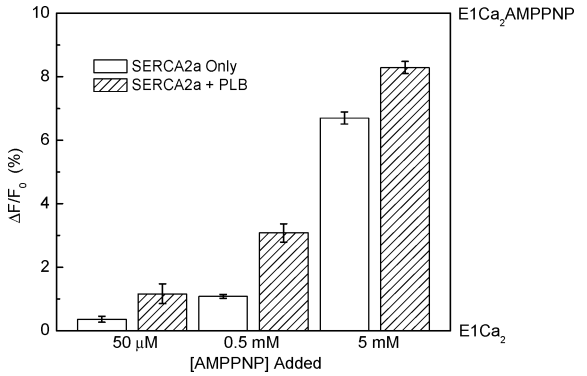

FIGURE 5: Effect of PLB on the E1·Ca_2 to E1·Ca_2·AMPPNP conformational equilibrium at 25 °C. Insect cell microsomes containing AEDANS-SERCA2a alone (open bars) or with PLB (hatched bars) were incubated in standard buffer containing 1.0 mM EGTA plus 1.0 mM $CaCl_2$ ($[Ca^{2+}]_{free}$ ~15 μM) to promote the formation of the E1·Ca_2 state. The steady-state fluorescence intensity of AEDANS-SERCA2a was measured before and after the addition of either 50 μM, 0.5 mM, or 5 mM AMPPNP to the solution to promote the formation of the E1·Ca_2·AMPPNP intermediate. The change in fluorescence (ΔF) following AMPPNP addition was plotted as a percentage of the initial fluorescence (F_o) before AMPPNP addition. Each bar represents the average of six experiments, and error bars represent the standard error of the mean.

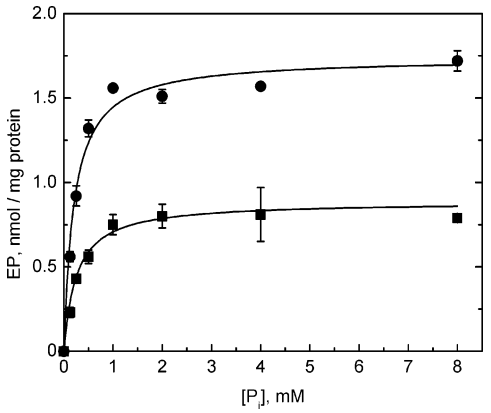

FIGURE 6: Effect of PLB on the [P_i] dependence of SERCA2a E2P formation at 25 °C. SERCA2a expressed in HF insect cell microsomes alone (●) or coexpressed with PLB in HF insect cell microsomes (■) were suspended (1.0 mg/mL) in a buffer containing 10 mM $MgCl_2$, 0 added $CaCl_2$ plus 1 mM EGTA ($[Ca^{2+}]_{free}$ ~ 0), and 50 mM MES at pH 6.0. To initiate the phosphorylation reaction, [^{32}P]Na_2HPO_4 in the same buffer was added to the samples to give the final concentrations as indicated. After incubation for 15 min at 25 °C, the reaction was quenched with 10% perchloric acid and processed for determination of ^{32}P-EP. The data were fit to a hyperbolic equation using KFIT (*30*) to generate values for K_{P_i} and $[EP]_{max}$ (Table 2). The symbols represent the average of four separate experiments, and error bars represent the standard error of the mean.

samples. The larger amplitude change in fluorescence for the PLB-containing sample following AMPPNP addition suggests that AMPPNP binding pulls an increased fraction of the enzyme from the PLB-stabilized state (Figures 3 and 4) to the E1·Ca_2 state and to E1·Ca_2·AMPPNP, relative to AEDANS-SERCA2a without PLB. In the absence of PLB, more of the enzyme is in the E1·Ca_2 state prior to AMPPNP addition, resulting in a smaller increase in fluorescence intensity.

[P_i]-Dependent EP Formation and [Ca^{2+}]-Dependent Inhibition of E2P Formation. In the absence of Ca^{2+}, P_i will phosphorylate the Ca-ATPase to form the E2P intermediate (*41*, *42*). We measured the effect of PLB on [P_i]-dependent EP formation at 25 °C for SERCA2a expressed alone or with PLB (Figure 6 and Table 2). The presence of PLB resulted in a 53% decrease ($p < 0.05$) in the maximum EP level and increased the K_{P_i} by 70 μM ($p < 0.05$), indicating that, in addition to inhibiting SERCA2a E2P formation from P_i, PLB decreased the apparent affinity of the enzyme for P_i. Ca-ATPase E2P formation from P_i is inhibited in presence of Ca^{2+}, because calcium converts the enzyme from E2 into E1·Ca_2, which does not react with P_i (*41*). We measured the effect of PLB on the [Ca^{2+}]-dependent inhibition of SERCA2a EP formation from P_i at 25 °C and found that PLB had no significant effect on this inhibition (Figure 7 and Table 2). Our results showing that PLB decreased the amplitude of EP formation by P_i are consistent with a PLB-dependent decrease in ATPase activity (Figure 1A) and the decreased amplitude of the SERCA2a E2 → E1·Ca_2 transition (Figures 3 and 4). However, the observation that PLB did not affect the $K_{0.5}$ for Ca^{2+}-dependent EP inhibition differs from that obtained in our activity and fluorescence studies. Together, these results suggest that PLB rather than Ca^{2+} controls the poise of the E2 + P_i ↔ E2P equilibrium, which is shifted away from E2P; increasing [Ca^{2+}] simply depletes the pool of E2 sites available for rephosphorylation by P_i.

SERCA2a Inhibition by Vanadate. Orthovanadate is a potent Ca-ATPase inhibitor that binds only to the E2 conformation and forms a transition-state analogue (E2V) of the E2P intermediate (*43*−*45*). We measured the effect of PLB on SERCA2a inhibition by vanadate (Figure 8) in the presence of 625 nM ionized [Ca^{2+}], arbitrarily selected to be near the average $K_{0.5}$ value for the two SERCA2a samples (Table 1). These experiments were carried out at 37 °C to maximize ATPase activity and increase the resolution of the vanadate-dependent loss of SERCA2a activity in the two samples. The data are shown normalized to allow for a direct comparison of the PLB-dependent difference in SERCA2a inhibition by vanadate. For both samples, complete enzyme inhibition was observed at 100 μM vanadate, which is typical for the Ca-ATPase (*46*, *47*). However, relative to SERCA2a in the absence of PLB [IC_{50} = 335 ± 60 nM (n = 4)], the presence of PLB (■ in Figure 8) shifted the SERCA2a inhibition curve to the right, significantly increasing ($p < 0.05$) the IC_{50} value [630 ± 50 nM (n = 4)]. Thus, PLB reduced SERCA2a sensitivity to vanadate. Because unphosphorylated PLB does not block the SERCA2a phosphorylation site (D351) (*5*, *23*), the results suggest that PLB binding to SERCA2a shifts the enzyme to a conformation that is not receptive to vanadate binding, i.e., a conformation that is distinct from the E2 form. This is

Table 2: [P_i]-Dependent EP Formation by Expressed SERCA2a in HF Insect Cell Microsomes[a]

	K_{P_i} (mM)	$[EP]_{max}$ (nmol/mg)	K_{Ca} (nM)
SERCA2a alone	0.20 ± 0.01	1.7 ± 0.1	750 ± 35
SERCA2a plus PLB	0.27 ± 0.01	0.80 ± 0.1	820 ± 70

[a] The [P_i]-dependent EP formation curves of Figure 6 were used to determine the [P_i] required for half-maximal phosphorylation (K_{P_i}) and the maximum EP level obtained ($[EP]_{max}$). The [Ca^{2+}]-dependent inhibition of SERCA2a EP formation (Figure 7) provided the [Ca^{2+}] required for half-maximal inhibition (K_{Ca}). Values represent the mean of four separate determinations for each sample type, and the errors represent the standard error of the mean.

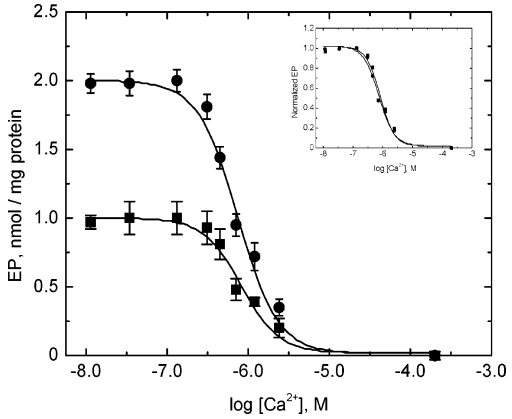

FIGURE 7: Effect of PLB on the $[Ca^{2+}]$-dependent inhibition of SERCA2a E2P formation at 25 °C. HF insect cell microsomes containing SERCA2a alone (●) or SERCA2a plus PLB (■) were suspended (1.0 mg/mL) in a buffer containing 10 mM $MgCl_2$, 1 mM EGTA plus 0 added $CaCl_2$ ($[Ca^{2+}]_{free} \sim 0$), and 50 mM MES at pH 6.0. To initiate the phosphorylation reaction, 4 mM $[^{32}P]Na_2HPO_4$ plus 0−1.2 mM $CaCl_2$ in the same buffer was added to the samples, to provide $[Ca^{2+}]_{free}$ levels between 0 and 200 μM in the reaction mixture. After incubation for 15 min at 25 °C, the reaction was quenched with acid and processed for determination of ^{32}P-EP levels. The inset shows the data sets normalized to their maximum EP level to facilitate a comparison of the two curves. The data were fit by the Hill equation using KFIT (*30*) to generate values for K_{Ca} (Table 2). The symbols represent the average of four separate experiment measurements, and error bars represent the standard error of the mean.

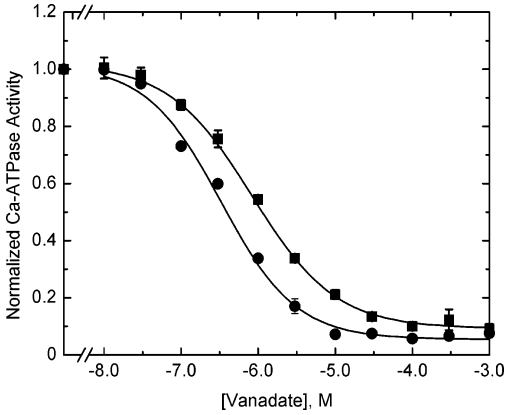

FIGURE 8: Effect of PLB on SERCA2a inhibition by vanadate at 37 °C. SERCA2a activity was measured as described in Figure 1, except that the $[CaCl_2]$ was fixed at 0.7 mM to provide a $[Ca^{2+}]_{free}$ of 625 nM. Samples were preincubated in the presence of the indicated levels of vanadate for 10 min at 37 °C prior to the start of the assay. The plot is shown normalized to offset PLB-dependent differences in SERCA2a activity and allow for a direct comparison of the [vanadate] dependence for each sample. The data were fit by the Hill equation using KFIT (*30*) to generate the IC_{50} values. Symbols represent the average of seven separate experiments, and error bars denote the standard error of the mean.

consistent with the results of the fluorescence (Figures 3 and 4) and phosphorylation (Figure 6) experiments, showing that PLB decreased the amplitude of conformational changes involving the E2 intermediate and decreased SERCA2a sensitivity to the ligands that promote these conformational changes.

DISCUSSION

The conformational transitions and protein−protein interactions of the skeletal muscle Ca-ATPase (SERCA1 isoform) have been studied extensively using the fluorescent probe IAEDANS in steady-state and stopped-flow fluorescence experiments (*36*, *38*, *49*) and fluorescence resonance energy transfer (FRET) experiments (*48*, *49*). More recently, IAEDANS-labeled SERCA1 has been used in FRET studies to measure the association of PLB with Ca-ATPase in various enzyme intermediate states (*16*). The present study represents an extension of this body of work to understand the effect of PLB on cardiac Ca-ATPase conformational changes and equilibria. Our IAEDANS SERCA2a labeling studies (Figures 2 and 4) confirmed that the expressed SERCA2a was the only protein in the insect cell microsomes that was significantly labeled by IAEDANS and that covalent attachment of the probe had no significant effects on the functional coupling or inhibitory interaction of PLB with the enzyme. We found that PLB decreased the amplitude of the E2 → E1·Ca_2 conformational transition (Figures 3A and 4A), consistent with the interpretation that PLB shifts the poise of the equilibrium away from E1·Ca_2, even at saturating Ca^{2+} levels. Our results showing that PLB increased the K_{Ca} for the $[Ca^{2+}]$ dependence of the SERCA2a E2 → E1·Ca_2 transition (Figure 4B) to the same extent as the PLB-dependent shift in the $[Ca^{2+}]$ dependence of enzyme activity (Figure 1B) supports the conclusion that PLB decreases SERCA2a apparent Ca^{2+} affinity by decreasing the population of enzyme E1 sites available for high-affinity Ca^{2+} binding and enzyme activation. Likewise, PLB decreased the amplitude of E2P formation by P_i (Figures 6 and 7), consistent with the interpretation that PLB decreased the level of E2 sites capable of binding P_i. The expressed SERCA2a protein content in the two sample types was carefully matched for these studies, suggesting that the PLB-dependent decrease in fluorescence amplitude and E2P formation did not result from differences in SERCA2a levels in the microsomes. These results suggest that PLB stabilizes SERCA2a in a conformation distinct from E2 and E1·Ca_2. Alternatively, it is possible that the observed differences in fluorescence intensity changes arose from PLB-dependent structural differences at the SERCA2a cysteine residue(s) labeled by AEDANS, resulting in fundamental differences in probe orientation and probe mobility in its local environment. This is unlikely, in that we found the same stoichiometry of labeling between the two sample types and $[Ca^{2+}]$- and [AMPPNP]-dependent fluorescence changes that were of similar magnitude between the two sample types and comparable to values previously reported in the literature (*36*, *38*, *39*). Therefore, we conclude that the fluorescence intensity changes that we measured reported PLB-dependent changes in SERCA2a conformation.

By definition, the Ca-ATPase E2 state is the Ca^{2+}-free form of the enzyme that is reactive toward P_i, monovanadate, and TG (*28*). Chemical cross-linking studies show that conditions favoring the formation of the E2 intermediate state (i.e., very low $[Ca^{2+}]$) increase the association of inhibitory (unphosphorylated) PLB with the enzyme, particularly in the presence of ATP (*18*, *19*), and are correlated with increased potency of PLB inhibition of SERCA2a. However, our results show that the PLB-associated enzyme is resistant to agents that bind specifically to the E2 state, suggesting the PLB-inhibited Ca-ATPase is in a conformation distinct from E2. Clearly, this conformation is not E1, because increasing $[Ca^{2+}]$, which favors E1 formation, diminishes the potency

of PLB inhibition of the enzyme (Figure 1) and decreases the site-specific cross-linking between PLB and Ca-ATPase observed in the absence of Ca^{2+} (*18*, *19*). Likewise, this conformation is not the E2·TG conformation (*28*), formed by the binding of TG to the enzyme E2. Mahaney et al. (*29*) showed that PLB decreases SERCA2a sensitivity to TG, and Jones and co-workers (*18*, *19*) showed that TG bound to SERCA2a prevents site-specific cross-linking between unphosphorylated PLB and SERCA2a. Li et al. (*26*) proposed that inhibitory PLB binding to the E2 form of SERCA2a induces a 10° reorientation of the N domain toward the bilayer (cf. Figure 8 of ref *24*), which traps the Ca-ATPase in a separate conformational state (designated as "E" in the present study), intermediate between the E2 and E1 forms of the enzyme. On the basis of this proposal, we developed a similar model (Figure 9) to account for our spectroscopic and kinetic data. In our model, inhibitory PLB bound to the Ca-ATPase reduces the number of enzymes in the E2 state capable of binding E2-specific ligands (P_i, vanadate, and TG), while also reducing the number of E1 enzyme units that can bind Ca^{2+} ions with high affinity. By mass action, Ca^{2+} binding to E1 will draw the enzyme away from the PLB·E state toward the E1·Ca_2 state, although higher Ca^{2+} levels will be required to reach the E1·Ca_2 state, giving the appearance of decreased Ca^{2+} affinity in the presence of inhibitory PLB. Likewise, increased levels of P_i, vanadate, or TG will be required to draw the enzyme into the E2P, E2V, or E2·TG state, respectively, manifesting as a decrease in the apparent affinity for each agent. Indeed, our results show that PLB increased the [Ca^{2+}] required for half-maximal E1·Ca_2 formation (Figure 1B), increased the [P_i] required for half-maximal E2P formation by P_i (Figure 6), and increased the IC_{50} value for SERCA2a inhibition by the P_i analogue, vanadate (Figure 8).

While the PLB-induced shifts in K_m and IC_{50} can be readily explained in terms of mass-action effects of the various ligands on the chemical equilibria in a simple model (Figure 9), the mechanism underlying the accompanying amplitude changes is not so transparent. An assumption is that the existence of PLB·E reduces the amplitude of the fluorescence changes starting either with the E1·Ca_2 state or with E2 stripped of Ca^{2+} and reduces the level of EP formation produced by the addition of saturating P_i. If the different states in the reaction pathway are in equilibrium, as shown in the model, then the addition of a ligand that binds tightly to E1 (e.g., Ca^{2+}) should pull on the equilibria connected to this state and deplete E2 and PLB·E to levels that will depend upon the magnitude of the rate constants of the competing reactions as well as the ligand concentrations (for second-order reactions). If we consider just the upper pathway in Figure 9

$$\text{PLB·E} \leftrightarrow {}_{\text{PLB}}\text{E1} + 2\text{Ca}^{2+} \leftrightarrow {}_{\text{PLB}}\text{E1·Ca}_2$$

then raising the [Ca^{2+}] to a saturating level should pull the enzyme into the intermediate on the right while depleting the intermediate on the left. For a significant amount (~45%; cf. Figure 3A) of the enzyme to remain in PLB·E under these conditions, the rate of formation of PLB·E from $_{PLB}$E1 must be competitive with Ca^{2+} binding to $_{PLB}$E1; in fact, the forward and reverse rate constants in each of the two steps are such that PLB·E and $_{PLB}$E1·Ca_2 exist in an approximately

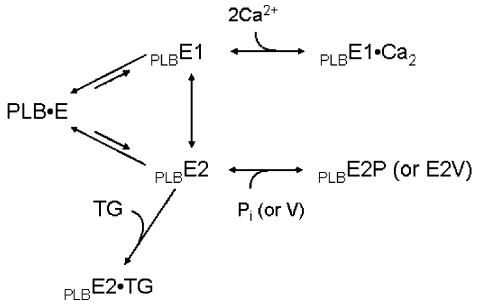

FIGURE 9: Model for PLB-dependent inhibition of SERCA2a conformational changes involving the E2 intermediate state. In the absence of the substrate or ligands, SERCA2a is in equilibrium between the E2 and E1 states. Ca^{2+} binding to its high-affinity sites on E1 will promote the formation of the E1·Ca_2 state, and in the presence of the ATP analogue, AMPPNP will progress to the E1·Ca_2·AMPPNP state (not shown). In the absence of Ca^{2+}, inorganic phosphate (P_i) or vanadate (V) will bind to the E2 state and promote the formation of the covalent E2P (or E2V) complex or TG will bind the E2 state to form the E2·TG state. Inhibitory PLB binding to the E2 state induces a reorientation of the nucleotide domain (*26*), forming a unique E2-like conformational state, designated "E". PLB interacts with all SERCA2a intermediate states (*13*, *14*), but the interaction is most potent when SERCA2a is in the E state (denoted by the large "PLB") and less potent (or nonpotent) for other SERCA2a intermediate states (denoted by small subscripted "PLB"). When SERCA2a units are drawn into the E state, PLB will deplete E2 units available to bind P_i (Figures 6 and 7), vanadate (Figure 8) or TG (*27*), while also reducing the number of E1 units with high-affinity Ca^{2+} (Figures 3 and 4) and AMPPNP (Figure 5) binding sites.

45:55 distribution at 15 μM free Ca^{2+}. In this situation, raising or lowering the free [Ca^{2+}] should perturb the equilibrium, decreasing or increasing the amount of PLB·E, respectively. Examination of the Ca^{2+} dependence of the AEDANS-SERCA2a fluorescence change (Figure 4A) suggests that the signal amplitude is rather stable in the [Ca^{2+}] range above 1 μM, which would argue against the simple equilibrium model shown above. The same quantitative argument can be raised with regard to the effects of [P_i] on enzyme phosphorylation as shown in Figure 6. In the presence of PLB, the SERCA2a EP levels remain relatively constant at ~0.8 nmol/mg of protein at concentrations between 1 and 8 mM P_i, demonstrating that the approximately 50:50 distribution of PLB·E and E2P at 1 mM P_i is not perturbed by a further increase in [P_i]. This suggests that additional SERCA2a physical factors beyond the simple mechanism shown in the lower pathway of Figure 9 are acting to stabilize PLB·E against conversion to E2P at high P_i concentrations.

We recently reported that inhibitory (unphosphorylated) PLB prevents SERCA2a oligomeric interactions important for high-affinity Ca^{2+} transport activity (*12*). Our study showed that, in the presence of inhibitory PLB, SERCA2a kinetics were characteristic of a functionally monomeric enzyme: (1) the E1P → E2P conformational transition is very rapid, resulting in a low steady-state level of E1P; and (2) E2P hydrolysis is very slow, resulting in a monophasic E2P decay pattern. Because the E2 ↔ E1 conformational equilibrium in the presence of PLB favors E2 (*18*, *19*), less high-affinity E1 sites are available for Ca^{2+} binding, resulting in a decrease in the apparent Ca^{2+} affinity ($\uparrow K_m$) of the enzyme. In the absence of PLB, SERCA2a oligomerizes into an asymmetric dimer, E1/E2, which, by conformational coupling, accelerates enzyme turnover by utilizing the free

energy liberated by the rapid E1P → E2P transition on one subunit to accelerate E2P hydrolysis on the other subunit. In effect, SERCA2a oligomer formation equalizes the populations of E1 and E2, increasing [E1] by a mass-action effect that increases the apparent Ca^{2+} affinity ($\downarrow K_m$) of the enzyme. This differs from the model of Cantilina et al. (*50*), in which the increase in the apparent Ca^{2+} affinity at the cytoplasmic transport sites arises from the relief of PLB-dependent inhibition of the forward and reverse rate constants of the conformational transition separating binding of the first and second Ca^{2+} ions. Their model predicts that relief of PLB inhibition will increase in the apparent rate of phosphorylation at subsaturating [Ca^{2+}], in contrast to the observations of Mahaney et al. (*37*), who found that the rate was unchanged in the presence or absence of PLB.

The apparent stability of PLB·E under conditions favoring its depletion (viz., increasing [Ca^{2+}] and [P_i]) suggests that oligomeric interactions involving SERCA2a and SERCA2a·PLB may exist prior to the relief of PLB inhibition leading to the activation of the Ca^{2+} pump. Consistent with this possibility, saturation transfer electron paramagnetic resonance (EPR) measurements with expressed SR proteins (*31*) and chemical cross-linking studies with native CSR (*14*) indicate the presence of SERCA2a oligomers in the absence of conditions that would relieve PLB inhibition. The presence of a tight oligomeric association between E1·Ca_2 and PLB·E (E1·Ca_2/PLB·E) or E2 and PLB·E (E2/PLB·E) might prevent the complete conversion of the dimeric species to one or the other principal conformational states following the addition of EGTA, Ca^{2+}, or P_i. In that case, the free energy of the intermolecular interaction exceeds the ligand-binding energy and stabilizes PLB·E, preventing its conversion to E1 or E2. When PLB inhibition is removed, say, in response to phosphorylation or by the addition of anti-PLB antibody, then the conversion of PLB·E to one of the principal conformational states can occur driven by ligand binding. To preserve the mass-action argument used above to explain the decrease in K_m upon activation of SERCA2a, it must be assumed that the total number of enzyme units in E2 and PLB·E (neither of which bind Ca^{2+}) exceeds those in E1. In this context, the enzyme conformational state in PLB·E resembles E2, so that upon relief of PLB inhibition and formation of the asymmetric dimer, E1/E2, the total population of enzyme in E1 increases relative to that in which PLB inhibition is present. The suggestion that PLB·E is stabilized against Ca^{2+} binding by virtue of its tight association with another subunit in an oligomer is reminiscent of the situation in native skeletal muscle SERCA1, where the total stoichiometry of Ca^{2+}-binding sites (7−8 nmol/mg of pump protein) (*52*) is roughly equivalent to the density of enzymatic sites (*52*, *53*). Because two Ca^{2+} ions bind per 100 kD polypeptide chain, only half of the subunits are occupied, leaving the other half in a conformational state that does not bind Ca^{2+}, presumably E2.

The results of the present study provide new insight into the effect of PLB on Ca-ATPase oligomeric interactions by showing that PLB stabilizes the enzyme in a conformational state that is structurally distinct from the E2 and E1·Ca_2 conformations and, therefore, may not efficiently couple with either the E2 or E1 states within an oligomeric complex. Coupling here implies a specific physical interaction between subunits within an oligomer that leads to a gain in free energy of activation with the acceleration of rate of one reaction in one subunit and the equivalent loss of free energy of activation and slowing of the rate of another reaction in an adjacent subunit. The results of the experiments where PLB was present are compatible with the existence of a SERCA2a oligomer in which the subunits are *associated* but not *chemically* coupled. In this scenario, activation of the system subsequent to the relief of PLB inhibition would entail conversion of the system from one in which the subunits are physically associated to one in which they are conformationally associated *and* chemically coupled. Our working hypothesis (*12*) is that the conformational change in PLB subsequent to its phosphorylation at Ser-16 (*5*, *54*) permits the association between the A and N domains of neighboring SERCA2a molecules at specific contact points, leading to conformational and chemical coupling. Additional spectroscopic and kinetic studies investigating the reversibility of the PLB-dependent effect through the use of PLB phosphorylation or treatment of the samples with anti-PLB monoclonal antibody will test this proposal more fully.

REFERENCES

1. Stokes, D. L., and Green, N. M. (2003) Structure and function of the calcium pump, *Annu. Rev. Biophys. Biomol. Struct. 32*, 445−468.
2. Toyoshima, C., and Inesi, G. (2004) Structural basis of ion pumping by Ca-ATPase of the sarcoplasmic reticulum, *Ann. Rev. Biochem. 73*, 269−292.
3. Simmerman, H. K., and Jones, L. R. (1998) Phospholamban: Protein structure, mechanism of action, and role in cardiac function, *Physiol. Rev. 78*, 921−947.
4. Frank, K., and Kranias, E. G. (2003) Phospholamban and cardiac contractility, *Ann. Med. 32*, 572−578.
5. Bigelow, D. J., and Squier, T. C. (2006) Coil-to-helix transition within phospholamban underlies release of Ca-ATPase inhibition in response to β-adrenergic signaling, *Curr. Enzyme Inhib. 2*, 19−27.
6. Hagemann, D., and Xiao, R. P. (2002) Dual site phospholamban phosphorylation and its physiological relevance in the heart, *Trends Cardiovasc. Med. 12*, 51−56.
7. Schmidt, A. G., Edes, I., and Kranias, E. G. (2001) Phospholamban: A promising therapeutic target in heart failure? *Cardiovasc. Drugs Ther. 15*, 387−396.
8. Frank, K. F., Bolck, B., Erdmann, E., and Schwinger, R. H. (2003) Sarcoplasmic reticulum Ca-ATPase modulates cardiac contraction and relaxation, *Cardiovasc. Res. 57*, 20−27.
9. MacLennan, D. H., and Kranias, E. G. (2003) Phospholamban: A crucial regulator of cardiac contractility, *Nat. Rev. Mol. Cell. Biol. 4*, 566−577.
10. Schmitt, J. P., Kamisago, M., Asahi, M., Li, G. H., Ahmad, F., Mende, U., Kranias, E. G., MacLennan, D. H., Seidman, J. G., and Seidman, C. E. (2003) Dilated cardiomyopathy and heart failure caused by a mutation in phospholamban, *Science 299*, 1410−1413.
11. Haghighi, K., Kolokathis, F., Pater, L., Lynch, R. A., Asahi, M., Gramolini, A. O., Fan, G. C., Tsiapras, D., Hahn, H. S., Adamopoulos, S., Liggett, S. B., Dorn, G. W., II, MacLennan, D. H., Kremastinos, D. T., and Kranias, E. G. (2003) Human phospholamban null results in lethal dilated cardiomyopathy revealing a critical difference between mouse and human, *J. Clin. Invest. 111*, 869−876.
12. Mahaney, J. E., Albers, R. W., Waggoner, J. R., Kutchai, H. C., and Froehlich, J. P. (2005) Intermolecular conformational coupling and free energy exchange enhance the catalytic efficiency of cardiac muscle SERCA2a following the relief of phospholamban inhibition, *Biochemistry 44*, 7713−7724.
13. Negash, S., Huang, S., and Squier, T. C. (1999) Rearrangement of domain elements of the Ca-ATPase in cardiac sarcoplasmic reticulum membranes upon phospholamban phosphorylation, *Biochemistry 38*, 8150−8158.

14. Lennon, N. J., Harmon, S., MacKey, A., and Ohlendieck, K. (1999) Oligomerization of the sarcoplasmic reticulum Ca^{2+}-ATPase SERCA2 in cardiac muscle, *Mol. Cell. Biol. Res. Commun. 1*, 182−187.
15. Tatulian, S. A., Chen, B., Li, J., Negash, S., Middaugh, C. R., Bigelow, D. J., and Squier, T. C. (2002) The inhibitory action of phospholamban involves stabilization of α-helices within the Ca-ATPase, *Biochemistry 41*, 741−751.
16. Mueller, B., Karim, C. B., Negrashov, I. V., Kutchai, H., and Thomas, D. D. (2004) Direct detection of phospholamban and sarcoplasmic reticulum Ca-ATPase interaction in membranes using fluorescence resonance energy transfer, *Biochemistry 43*, 8754−8765.
17. Negash, S., Yao, Q., Sun, H., Li, J., Bigelow, D. J., and Squier, T. C. (2000) Phospholamban remains associated with the Ca^{2+}- and Mg^{2+}-dependent ATPase following phosphorylation by cAMP-dependent protein kinase, *Biochem. J. 351*, 195−205.
18. Jones, L. R., Cornea, R. L., and Chen, Z. (2002) Close proximity between residue 30 of phospholamban and cysteine 318 of the cardiac Ca^{2+} pump revealed by intermolecular thiol cross-linking, *J. Biol. Chem. 277*, 28319−28329.
19. Chen, Z., Stokes, D. L., Rice, W. J., and Jones, L. R. (2003) Spatial and dynamic interactions between phospholamban and the canine cardiac Ca^{2+} pump revealed with use of heterobifunctional cross-linking agents, *J. Biol. Chem. 278*, 48348−48356.
20. Chen, Z., Stokes, D. L., and Jones, L. R. (2005) Role of leucine 31 of phospholamban in structural and functional interactions with the Ca^{2+} pump of cardiac sarcoplasmic reticulum, *J. Biol. Chem. 280*, 10530−10539.
21. Hutter, M. C., Krebs, J., Meiler, J., Griesinger, C., Carafoli, E., and Helms, V. (2002) A structural model of the complex formed by phospholamban and the calcium pump of sarcoplasmic reticulum obtained by molecular mechanics, *ChemBioChem 3*, 1200−1208.
22. Toyoshima, C., Asahi, M., Sugita, Y., Khanna, R., Tsuda, T., and MacLennan, D. H. (2003) Modeling of the inhibitory interaction of phospholamban with the Ca^{2+}-ATPase, *Proc. Natl. Acad. Sci. U.S.A. 100*, 467−472.
23. Zamoon, J., Nitu, F., Karim, C., Thomas, D. D., and Veglia, G. (2005) Mapping the interaction surface of a membrane protein: Unveiling the conformational switch of phospholamban in calcium pump regulation, *Proc. Natl. Acad. Sci. U.S.A. 102*, 4747−4752.
24. Li, J., Bigelow, D. J., and Squier, T. C. (2003) Phosphorylation by cAMP-dependent protein kinase modulates the structural coupling between the transmembrane and cytosolic domains of phospholamban, *Biochemistry 42*, 10674−10682.
25. Li, J., Xiong, Y., Bigelow, D. J., and Squier, T. C. (2004) Phospholamban binds in a compact and ordered conformation to the Ca-ATPase, *Biochemistry 43*, 455−463.
26. Li, J., Bigelow, D. J., and Squier, T. C. (2004) Conformational changes within the cytosolic portion of phospholamban upon release of Ca-ATPase inhibition, *Biochemistry 43*, 3870−3879.
27. Toyoshima, C., Nakasako, M., Nomura, H., and Ogawa, H. (2000) Crystal structure of the calcium pump of sarcoplasmic reticulum at 2.6 Å resolution, *Nature 405*, 647−655.
28. Toyoshima, C., and Nomura, H. (2002) Structural changes in the calcium pump accompanying the dissociation of calcium, *Nature 418*, 605−611.
29. Mahaney, J., Barlow, A., Honaker, B., Huffman, J., and Muchnok, T. (1999) Phospholamban reduces cardiac Ca-ATPase sensitivity to thapsigargin and cyclopiazonic acid, *Arch. Biochem. Biophys. 372*, 408−413.
30. Waggoner, J. R., Huffman, J., Griffith, B. N., Jones, L. R., and Mahaney, J. E. (2004) Improved expression and characterization of Ca-ATPase and phospholamban in High-Five cells, *Protein Expression Purif. 34*, 56−67.
31. Mahaney, J. E., Albers, R. W., Kutchai, H., and Froehlich, J. P. (2003) Phospholamban controls Ca^{2+} pump oligomerization and intersubunit free energy exchange leading to activation of cardiac muscle SERCA2a, *Ann. N.Y. Acad. Sci. 986*, 1−3.
32. Lowry, O., Rosebrough, N., Farr, A., and Randall, R. (1951) Protein measurement with the Folin phenol reagent, *J. Biol. Chem. 193*, 265−275.
33. Lanzetta, P. A., Alvarez, L. J., Reinach, P. S., and Candia, O. A. (1979) An improved assay for nanomole amounts of inorganic phosphate, *Anal. Biochem. 100*, 95−97.
34. Autry, J. M., and Jones, L. R. (1997) Functional Co-expression of the canine cardiac Ca^{2+} pump and phospholamban in *Spodoptera frugiperda* (Sf21) cells reveals new insights on ATPase regulation, *J. Biol. Chem. 272*, 15872−15880.
35. Goodno, C. C. (1982) Myosin active-site trapping with vanadate ion, *Methods Enzymol. 85*, 116−123.
36. Obara, M., Suzuki, H., and Kanazawa, T. (1988) Conformational changes in the vicinity of the *N*-iodoacetyl-*N*′-(5-sulfo-1-naphthyl)-ethylenediamine attached to the specific thiol of sarcoplasmic reticulum Ca-ATPase throughout the catalytic cycle, *J. Biol. Chem. 263*, 3690−3697.
37. Mahaney, J. E., Autry, J. M., and Jones, L. R. (2000) Kinetics studies of the cardiac Ca-ATPase expressed in Sf21 cells: New insights on Ca-ATPase regulation by phospholamban, *Biophys. J. 78*, 1306−1323.
38. Suzuki, H., Obara, M., Kubo, K., and Kanazawa, T. (1989) Changes in the steady-state fluorescence anisotropy of *N*-iodoacetyl-*N*′-(5-sulfo-1-naphthyl)ethylenediamine attached to the specific thiol of sarcoplasmic reticulum Ca^{2+}-ATPase throughout the catalytic cycle, *J. Biol. Chem. 264*, 920−927.
39. Suzuki, H., Obara, M., Kuwayama, H., and Kanazawa, T. (1987) A conformational change of *N*-iodoacetyl-*N*′-(5-sulfo-1-naphthyl)-ethylenediamine-labeled sarcoplasmic reticulum Ca^{2+}-ATPase upon ATP binding to the catalytic site, *J. Biol. Chem. 262*, 15448−15456.
40. Mahaney, J. E., Froehlich, J. P., and Thomas, D. D. (1995) Conformational transitions of the sarcoplasmic reticulum Ca-ATPase studied by time-resolved EPR and quenched-flow kinetics, *Biochemistry 34*, 4864−4879.
41. Masuda, H., and de Meis, L. (1973) Phosphorylation of the sarcoplasmic reticulum membrane by orthophosphate inhibition by calcium ions, *Biochemistry 12*, 4581−4585.
42. Kanazawa, T., and Boyer, P. D. (1973) Occurrence and characteristics of a rapid exchange of phosphate oxygens catalyzed by sarcoplasmic reticulum vesicles, *J. Biol. Chem. 248*, 3163−3172.
43. Pick, U. (1982) The interaction of vanadate ions with the Ca-ATPase from sarcoplasmic reticulum, *J. Biol. Chem. 257*, 6111−6119.
44. Barrabin, H., and de Meis, L. (1982) Vanadate inhibition of the Ca-ATPase activity of sarcoplasmic reticulum vesicles, *An. Acad. Bras. Cienc. 54*, 743−751.
45. Inesi, G., Lewis, D., and Murphy, A. J. (1984) Interdependence of H^+, Ca^{2+}, and P_i (or vanadate) sites in sarcoplasmic reticulum ATPase, *J. Biol. Chem.* 259, 996−1003.
46. Wang, T., Tsai, L.-I., Solaro, R. J., Grassi de Gende, A. O., and Schwartz, A. (1979) Effects of potassium on vanadate inhibition of sarcoplasmic reticulum Ca^{2+}-ATPase from dog cardiac and rabbit skeletal muscle, *Biochem. Biophys. Res. Commun. 91*, 356−361.
47. Wierichs, R., Hagenmeyer, A., and Bader, H. (1980) Influence of Ca^{2+} and Mg^{2+} on the vanadate inhibition of the Ca^{2+}-ATPase from pig heart sarcoplasmic reticulum, *Biochem. Biophys. Res. Commun. 92*, 1124−1129.
48. Bigelow, D. J., Squier, T. C., and Inesi, G. (1992) Phosphorylation-dependent changes in the spatial relationship between Ca-ATPase polypeptide chains in sarcoplasmic reticulum membranes, *J. Biol. Chem. 267*, 6952−6962.
49. Squier, T. C., Bigelow, D. J., Garcia de Ancos, J., and Inesi, G. (1987) Localization of site-specific probes on the Ca-ATPase of sarcoplasmic reticulum using fluorescence energy transfer, *J. Biol. Chem. 262*, 4748−4754.
50. Cantilina, T., Sagara, Y., Inesi, G., and Jones, L. R. (1993) Comparative studies of cardiac and skeletal sarcoplasmic reticulum ATPases. Effect of a phospholamban antibody on enzyme activation by Ca^{2+}, *J. Biol. Chem. 268*, 17018−17025.
51. Inesi, G., Kurzmack, M., Coan, C., and Lewis, D. (1980) Cooperative calcium binding and ATPase activation in sarcoplasmic reticulum vesicles, *J. Biol. Chem. 255*, 3025−3031.
52. Warren, G. B., Toom, P. A., Birdsall, N. J. M., Lee, A. G., and Metcalfe, J. C. (1974) Reconstitution of a calcium pump using defined membrane components, *Proc. Nat. Acad. Sci. U.S.A. 71*, 622−626.
53. Froehlich, J. P., and Taylor, E. W. (1975) Transient state kinetic studies of sarcoplasmic reticulum adenosine triphosphatase, *J. Biol. Chem. 250*, 2013−2021.
54. Karim, C. B., Zhang, Z., Howard, E. C., Torgersen, K. D., and Thomas, D. D. (2006) Phosphorylation-dependent conformational switch in spin-labeled phospholamban bound to SERCA, *J. Mol. Biol. 358*, 1032−1040.

BI061365K